Talanta 81 (2010) 1069–1075

Contents lists available at ScienceDirect

Talanta

journal homepage: www.elsevier.com/locate/talanta

Fabrication of low-melting-point alloy microelectrode and monolithic spray tip for integration of glass chip with electrospray ionization mass spectrometry

Ying Zhu [a], Jian-Zhang Pan [a], Yuan Su [a], Qiao-Hong He [a], Qun Fang [a,b,*]

[a] Institute of Microanalytical Systems, Department of Chemistry, Zhejiang University, Hangzhou, China
[b] Key Laboratory for Biomedical Engineering of Ministry of Education of China, Zhejiang University, Hangzhou, China

ARTICLE INFO

Article history:
Received 23 November 2009
Received in revised form 25 January 2010
Accepted 28 January 2010
Available online 6 February 2010

Keywords:
Low-melting-point alloy
Electrospray ionization mass spectrometry
Glass chip
Monolithic emitter

ABSTRACT

In this paper, a glass microchip-based emitter with a low-melting-point alloy (LMA) microelectrode and a monolithic tip for electrospray ionization mass spectrometry (ESI-MS) was described. So far, the fabrication of metal microelectrode achieving direct electrical contact in the microchannel of glass chip is still a challenge. A novel fabrication approach for LMA microelectrode in the glass chip was developed to achieve direct electrode–solution electrical contact in the microchannel. An electrode channel and a sample channel were firstly fabricated on a glass chip with a micropore connecting the two channels. The melted LMA was filled into the electrode channel under a pressure of *ca.* 100 kPa, forming a stable and nicely fitted interface at the micropore between the sample and the electrode channels due to surface tension effect. The melted LMA filled in the electrode channel was then allowed to solidify at room temperature. The channel geometries including the distance between the sample and the electrode channels on the mask and the turning angle of the electrode channel were optimized for fabricating the LMA electrode. In this work, an improved fabrication approach for monolithic emitter tip based on pyramid-shaped tip configuration and stepped grinding method was also developed to fabricate well-defined sharp tips with a smallest tip end size of *ca.* 15 μm × 50 μm. Two types of emitter tip end including puncher-shaped tip and fork-shaped tip were produced. The emitter with the fork-shaped tip showed better working stability (4.4% RSD, TIC) at nanoliter-scale flow rate of 50 nL/min. The fabrication approaches for the LMA microelectrode and emitter tip are simple and robust, and could be carried out in most of routine laboratories without the need of complicated and expensive instruments. The performance of the emitter was evaluated in the analysis of reserpine, angiotensin II and myoglobin. A continuous experiment over 6 h demonstrated good stability of the present system in long-term analysis.

1. Introduction

The past decade has witnessed the rapid development of microfluidic chip-based analytical systems [1,2]. Various detection techniques, including absorbance and fluorescence detection [3,4], electrochemistry [5] and mass spectrometry (MS) [6,7] have been applied in these systems. MS detection technique has advantages of good versatility for different types of analytes, relatively high sensitivity and strong capability in molecule structural interpretation. In recent years, electrospray ionization mass spectrometry (ESI-MS) has become a major MS detection technique used in microfluidic chips due to its favorable ability in performing on-line detection [6,7].

Various approaches have been developed to achieve the combination of microchips and ESI-MS. Pioneered by Karger's group and Ramsey's group [8,9], the coupling of microchips with ESI-MS was firstly realized in a simple manner, by which the high voltage for electrospray was applied between the sample reservoir and the MS inlet orifice, and the electrospray was directly generated at the microchannel outlet on the flat edge of the chip. Later, microchip-based emitters for ESI-MS using a capillary emitter connected with the chip microchannel were developed [10–20]. In these emitters, the fabrication of spray tips and the electrical contact were easily achieved using the well-established technique for conventional capillary emitters. However, the relatively large dead volume existing at the junction of the chip microchannel and the capillary inlet in this type of emitter may lead to evident sample plug broadening when performing capillary electrophoresis separation on the microchip [6,21]. Thus, the development of on-chip monolithic emitters without dead volume has attracted more attention.

Currently, most of the on-chip monolithic electrospray emitters were fabricated based on plastic materials [22–30]. The electrical

* Corresponding author at: Institute of Microanalytical Systems, Chemistry Experiment Building, Room 101, Zhejiang University (Zijingang Campus), Hangzhou 310058, China. Tel.: +86 571 88206771; fax: +86 571 88273572.
E-mail address: fangqun@zju.edu.cn (Q. Fang).

0039-9140/$ – see front matter © 2010 Elsevier B.V. All rights reserved.
doi:10.1016/j.talanta.2010.01.064

contact in these emitters was realized using microfabricated electrode [23], conductive material coating [25], or embedded platinum wire [29]. Due to the simplicity in fabrication of plastic materials, well-defined monolithic spray tips could be easily produced using blade cutting [22,24], injection molding [26], laser ablation [27] or micromilling [25,28] techniques. Compared with plastic materials, glass has good chemical inertness and thermostability, and thus the ESI-MS emitters made from glass could provide much lower mass background level and higher detection sensitivity [30]. However, the fabrication of monolithic glass emitters for ESI-MS was quite difficult in both construction of electrical contact and fabrication of emitter tip [7,31], owing to the high hardness and brittleness properties of glass. Recently, several approaches have been proposed to address this challenge [31–33]. Yue et al. [32] used an etched glass membrane (20–50 μm in thickness) to conduct high voltage to sample solution. Hoffman et al. [31] described an approach using a computerized numerical control machine and a home-built heating puller to produce monolithic glass spray tips. During the preparation of this manuscript, Mellors et al. [33] developed a 300-μm thick glass chip for CE-ESI-MS, in which the potential was applied to the end of separation channel via a sheath flow channel and electrospray was generated directly at the corner of the rectangular chip.

In this work, a glass chip-based monolithic emitter for ESI-MS was developed. A novel fabrication approach for direct electrical-contact microelectrode on microchip was proposed using low-melting-point alloy (LMA). The fabrication technique of LMA microelectrode on microchip was firstly described by Whitesides' group to fabricate on-chip contactless electrodes, which functioned as electromagnets for the manipulation of magnetic microspheres [34]. In the present system, this technique was further explored, and for the first time applied to fabricate microelectrode for achieving direct electrode–solution contact in the chip-based emitter for ESI-MS. For the fabrication of the chip-based emitter tip, an improved fabrication approach was developed to fabricate well-defined sharp tips with a smallest tip end size of *ca.* 15 μm × 50 μm. The fabrication approaches for microelectrode and emitter tip are simple and robust, and could be carried out in most of routine laboratories. The performance of the chip-based emitter was evaluated in the analysis of reserpine, human angiotensin and myoglobin.

2. Experimental

2.1. Reagents and materials

Deionized water prepared with Millipore Ultrapure Water Systems (Billerica, USA) was used throughout. HPLC-grade methanol was purchased from Merck (Darmstadt, Germany), and glacial acetic acid was from TEDIA (Fairfield, USA). Reserpine, human angiotensin II, and horse myoglobin were products of Sigma–Aldrich (St. Louis, USA). Octadecyltrichlorosilane (ODS) was bought from Acros (Fair Lawn, USA).

2.2. Fabrication of glass chips

The mask design for the microchannels is illustrated in Figs. 1A and 2A, including a straight sample channel (10 μm width) and a V-shaped electrode channel (50 μm width). The distance *D* between the two channels was 30 μm unless mentioned otherwise. The turning angle of the V-shaped channel was 160°. Standard photolithographic and wet chemical etching techniques were used to fabricate microchannels on glass plate as described elsewhere [35]. After a 15-min wet etching process, the tip end of the V-shaped electrode channel (20 μm depth, 90 μm width) was connected to the sample channel (20 μm depth, 50 μm width) via a micropore

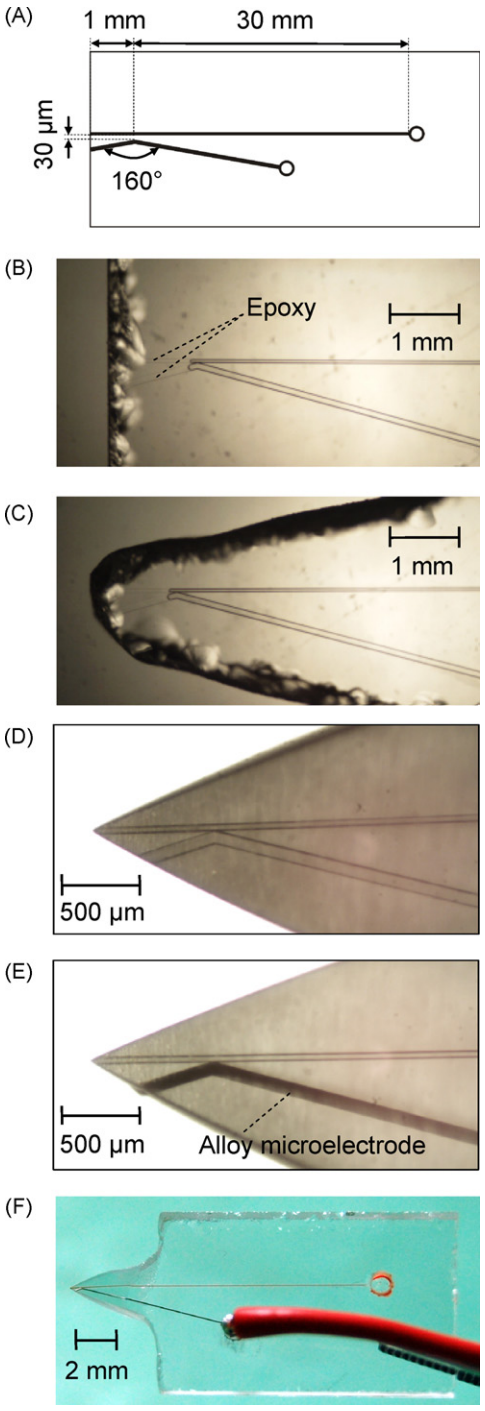

Fig. 1. Mask design for the microchannels on chip (A), CCD images of the ESI emitter chip during fabrication process (B–E) and the final appearance of the chip (F).

(Fig. 2B). Room-temperature pre-bonding and high-temperature (560 °C) bonding techniques were used to achieve the bonding of the cover and etched plates [36].

2.3. Fabrication of monolithic tips

Fig. 1B–D shows the fabrication process of the monolithic tip. Before fabrication, the outlet end of the channels was preblocked with epoxy to avoid clogging during the fabrication process (Fig. 1B). A relatively large tip (Fig. 1C) with a diameter of about 1 mm was first produced using an emery drill to grind the glass chips [37]. The tip was further ground into a pyramid shape by sequen-

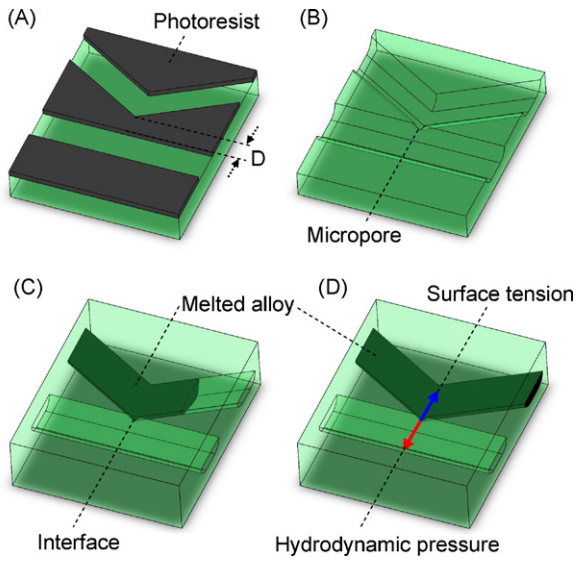

Fig. 2. Schematic diagram of the fabrication process of the LMA electrode (not to scale); photomask design for the microelectrode (A); after wet etching, the two channels connect with each other via a micropore (B); melted alloy flows into the electrode channel under external pressure (C); stable and nicely fitted phase interface forms at the micropore (D).

tially using waterproof sandpapers with 300, 600, and 2000 grid (Noon Decoration Material Co., Shanghai, China). The sandpapers were placed horizontally on a 2-cm high plastic platform. Four side walls of the pyramid-shaped tip were sequentially ground on the sandpaper with an angle of about 10° between the sample channel on the chip and the sandpaper. During the grinding process, water was continuously added to the tip to make the sample channel easily observed, ensuring the sample channel always located at the center of the tip. A stereomicroscope (ST60-24T2, Ningbo Sunny Instruments Co., China) equipped with a CCD camera (UMD200, Superimage Digital Technology Exploitation Co., Hangzhou, China) was used for fabrication process monitoring and image recording. After the grinding operation, the epoxy in the channel was removed by heating the chip in a muffle furnace (500 °C) for 1 h (Fig. 1D).

2.4. Fabrication of microelectrodes

The glass chip was placed on a home-made hotplate set at 140 °C. A simple gas pressure generator was made using a 1-mL plastic syringe by replacing the metal needle with a 1-cm long elastomeric tubing (3 mm i.d., 5 mm o.d.). Gas pressure was generated in the range of 100–500 kPa by compressing the gas in the syringe. A common type of LMAs, solder with melting point of 97 °C (composition of bismuth, tin and cadmium, Youbang Solder Metals Co., Hangzhou, China) was used to produce the electrode. The melted alloy (*ca.* 20 μL) was added into the inlet hole of the electrode channel and perfused into the whole electrode channel by applying a gas pressure of 100 kPa at the inlet (Fig. 2C), forming a stable and nicely fitted phase interface at the micropore between the electrode and the sample channels based on surface tension effect (Figs. 1E and 2D). A 5-cm long copper conducting wire was inserted into the alloy filled in the inlet hole, and then the chip was removed from the hotplate allowing the melted alloy to solidify at room temperature for 5 min. The surface of the tip outer wall was silanized with octadecyltrichlorosilane as described previously [38]. The completed emitter chip with a spray tip and LMA electrode is shown in Fig. 1F.

2.5. Fabrication of capillary emitters

In the comparison experiment, capillary emitters made from fused-silica capillaries (150 μm i.d., 365 μm o.d., Reafine Chromatography Co., Yongnian, China) were employed. The fused-silica capillary was heated to the melting state with a butane lighter and then was drawn manually. The capillary was cut in proper position using a ceramic cutter to form a tapered tip with a tip end size of approximately 50 μm i.d. and 120 μm o.d., which was similar to that of the on-chip emitter tip. The pulled capillary tip was polished under a stereomicroscope to ensure a flat tip end.

2.6. Mass spectrometry

All of the MS experiments were performed on an ion trap mass spectrometer (LCQ DECA XP, Thermo-Fisher Scientific Inc., Waltham, USA). The microchip was horizontally fixed on a three-dimensional translation stage (Daheng New Epoch Technology Inc., Beijing, China), and placed at a distance of 2 mm between the emitter tip end and the MS inlet orifice. The MS instrument was operated in "Tune Plus" view and was automatically tuned in all ESI-MS experiments. The heated capillary of the MS was set to a temperature of 200 °C. The ESI voltage was optimized in the range of 2000–2500 V. Each scan of mass spectra was summed of three microscans with a maximum injection time of 50 ms. A syringe pump (Harvard Picoplus, Holliston, USA) with a 100-μL syringe was used to deliver sample solution to the sample channel at flow rates in the range of 50–500 nL/min via a 10-cm long PTFE tubing (0.30 mm i.d., 0.76 mm o.d.). All of the samples were dissolved in the aqueous buffer of 50% methanol containing 1% acetic acid unless mentioned otherwise.

2.7. Microscope examinations

Scan Electron Microscope (S-570, Hitachi, Japan) was used to image the emitter tips. For the visualization of Taylor cone generated at the tip end of the emitters, the microchip was mounted on the platform of an inverted microscope (ECLIPSE TE-2000-S, Nikon Corporation, Japan) equipped with a CCD camera (SPOT RT-SE6 Monochrome, Diagnostic Instruments, USA).

3. Results and discussion

3.1. Low-melting-point alloy microelectrode

Hitherto, three approaches including the uses of conductive coatings on the outer surface of the spray tip end [11,14], porous glass junctions in the microchannel [32] and liquid junction with sheath flow [12,13,17,18,33], were mainly adopted in glass chip-based ESI-MS emitters to achieve electrical contact with sample solution. However, to our best knowledge, the approaches of fabricating on-chip metal microelectrodes widely used in polymer chips were seldom adopted in glass chips. The main challenge of integrating metal microelectrode on glass chip lay in the difficulty of achieving the bonding between a substrate with bossed microelectrodes and a flat cover plate.

In this work, we developed a simple and reliable approach to fabricate metal electrodes in microchannel network of glass chips using LMA molding technique. The melted LMA (usually with melting points below 200 °C) was perfused into the electrode channel and molded into a solid electrode which could directly contact the solution in the sample channel. Since the electrode was fabricated after the chip bonding, the difficulty in achieving bonding of substrates with integrated microelectrodes could be avoided. Compared with the emitters with porous glass junctions [32], the

present emitter capable of realizing direct electrode–solution contact allowed more stable electrospray performance under relatively lower high voltage. Another main advantage of the present fabrication approach was that the position of the electrode could be easily adjusted by designing different masks. In some emitters integrated with high-resolution separation systems, such as capillary electrophoresis, in order to minimize possible band broadening caused by Taylor dispersion and longitudinal diffusion, the electrical contact point should be chosen as close to spray tip end as possible [33]. This could be easily achieved with the present approach by reducing the distance between the electrical contact point and the tip end during the tip fabrication process. In addition to these, the LMA microelectrode in the present emitter had much longer working lifetime than those of thin layer electrodes with a nanometer-scale-thick metal coating on the outer surface of the emitters [25].

3.2. Optimization of fabrication process for the LMA microelectrode

In the fabrication process of the LMA electrode, one of the essential operations was to form a stable phase interface at the junction region between the electrode and the sample channels. To achieve such a goal, the principle of surface tension valve [39] was adopted by fabricating a V-shaped electrode channel which could connect to the sample channel with a micropore at their junction region. Below a certain threshold driving pressure, the surface tension of the melted LMA at the junction region could counteract the hydrodynamic pressure in the electrode channel (Fig. 2D), ensuring the formation of a stable and nicely fitted phase interface of the melted LMA at the micropore, as well as the continuously flowing out of the excess melted LMA from the outlet of the electrode channel. When the driving pressure exceeded the threshold value (namely leakage pressure), the melted LMA would leak from the electrode channel into the sample channel.

The size of the micropore between the electrode and the sample channels as well as the turning angle of the V-shaped electrode channel were found to have significant effects on the formation of phase interface of the melted LMA. The size of the micropore was decided by distance D (Figs. 1A and 2A) and the wet etching time due to the isotropic etching of glass. The effect of distance D on the leakage pressure was investigated with fixed wet etching time of 15 min. The leakage pressures were measured using a microscope to monitor the leakage of the melted LMA by gradually increasing the driving pressure. The results are shown in Fig. 3A. The leakage pressure significantly increased with the increase of distance D in the range of 0–40 μm, *i.e.* the decrease of the size of the micropore. Such results can be qualitatively explained using the Young–Laplace equation:

$$\Delta P = \frac{2\gamma}{R} = \frac{2\gamma \ \sin(\theta - 90^\circ)}{Rm}$$

where the ΔP is the surface tension across the melted LMA–air interface, γ the surface energy per unit area, θ the contact angle of the melted LMA on glass surface (measured as 120° at a temperature of 140 °C), and Rm the equivalent radius of the micropore between the two channels, which is decided by the micropore size. These parameters are illustrated in Fig. 3B. In the present system, γ and θ are constants, and Rm decreases with the increase of distance D. Therefore, the increasing trend of the surface tension with the increase of distance D could be deduced, which agrees with the experimental results.

The influence of the turning angle of the V-shaped electrode channel on the mask was also investigated with a fixed distance D of 30 μm and etching time of 15 min. Fig. 3C1–C3 shows three images of the electrode channels filled with melted LMA with turning angles of 45°, 90° and 160°, respectively, which were obtained

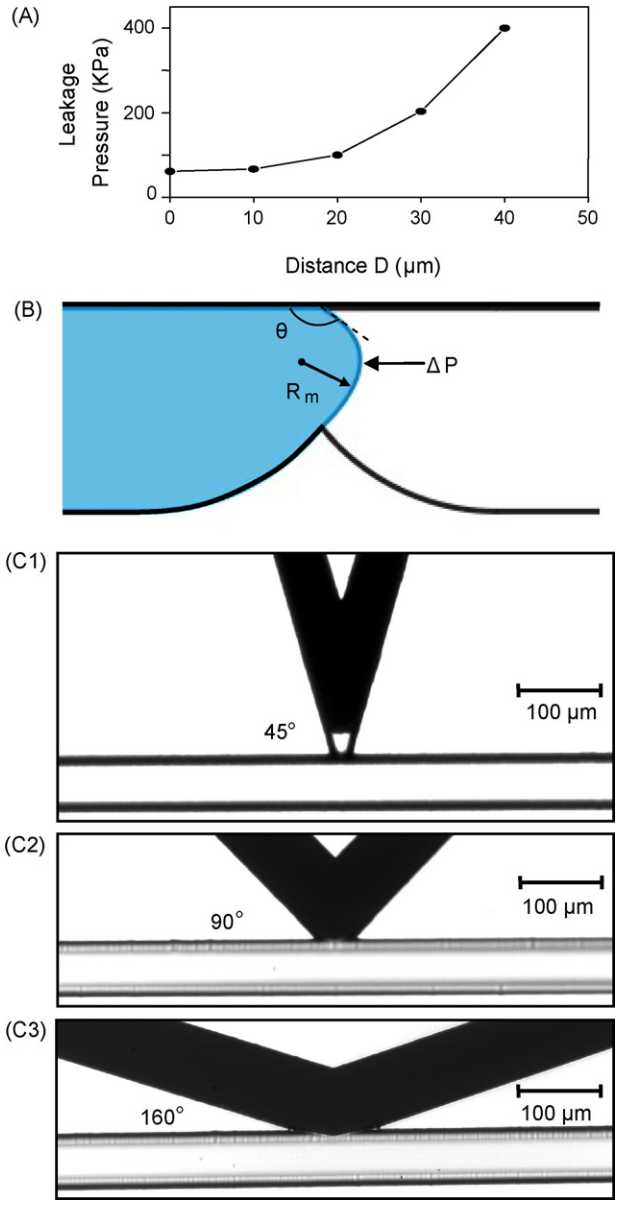

Fig. 3. Relationship between the leakage pressures of the melted LMA and the distance D (A); schematic illustration of the state of LMA at the micropore (B); images of the junction region between the sample channel and the V-shaped electrode channel with turning angles of 45° (C1), 90° (C2) and 160° (C3), with the melted alloy filled in the electrode channel.

under the same driving pressure of 100 kPa. The increase of the turning angle extended both widths of the tip channel of the V-shaped electrode channel and the micropore between the electrode and the sample channels. With turning angle of 45°, an obvious dead space for the melted LMA existed at the tip end of the electrode channel (Fig. 3C1), which could be attributed to the narrow tip channel and large surface tension of the melted LMA. With turning angle of 90° and 160°, stable and nicely fitted interfaces of the melted LMA could be formed at the micropore (Fig. 3C2 and C3) due to the relatively wide tip channel and micropore. Therefore, turning angle of 160° was used in the following experiments.

3.3. Monolithic spray tip

Monolithic spray tip was more attractive over capillary tip connected with chip channel because it eliminated the dead volume

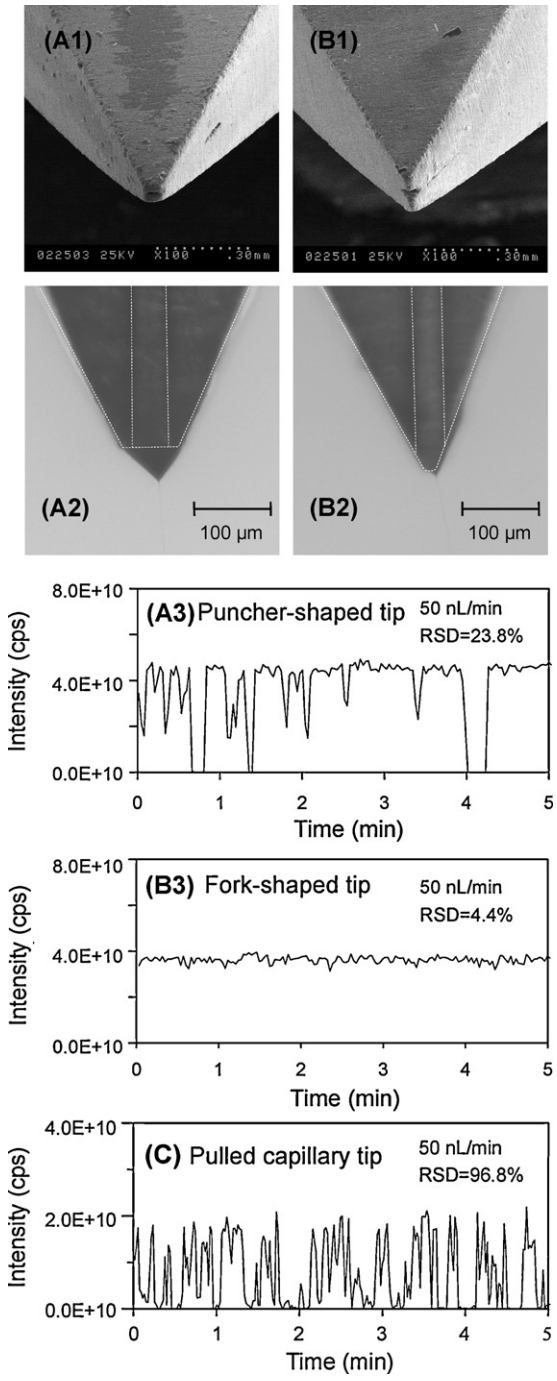

Fig. 4. SEM images of ESI emitters with a puncher-shaped tip (A1) and fork-like tip (B1), and the corresponding CCD images of Taylor cone (A2) and (B2). Typical total ion current (TIC) traces (10 μM myoglobin) from the puncher-shaped tip (A3), fork-like tip (B3) and the home-made pulled capillary tip (C); ESI voltage, 2.5 kV; infusion flow rate in (A2), (B2) and (C), 200 nL/min.

at the capillary–chip junction. However, due to the high hardness and brittleness properties of glass, producing a sharp tip on glass chip was still an issue. In the previous studies, we developed a fabrication approach for monolithic sampling probe on glass chip for automated sample introduction with tip diameters of *ca.* 400 μm [37]. However, such tip sizes could not match the requirement of micro-electrospray usually with tip sizes below 100 μm. Here, we further developed the fabrication technique using pyramid-shaped tip configuration and stepped grinding method to reduce the tip size to *ca.* 15 μm × 50 μm.

One of the challenges in the tip fabrication was to maintain the sample channel in the center of the tip, because the outer surface of the tip became rough and opaque due to the grinding operation. Water was added at the tip throughout the grinding process to increase the transparency of the tip and cool the chip. A 40× stereomicroscope was used to continuously monitor the grinding operation. Instead of taper-shaped tips used in the previous work [37], pyramid-shaped configuration for the spray tip was employed, which allowed the grinding operation and the position of the sample channel to be easily observed and precisely controlled.

Another challenge in the tip fabrication was to avoid the breakage of the tip end, especially when the size of the tip end was below 100 μm. Several approaches were adopted to ensure the success of the fabrication. First, the grinding operation was carried out along axial direction of the tip with grinding angles less than 20°. Such an approach avoided the grinding operation from producing large radial pressure on the tip which might break the tip end. Second, the pyramid configuration of the tip was also in favor of reducing the chance of it being broken due to the protecting effect of its thicker base to its thinner tip end. Third, the stepped grinding procedure was used to further reduce the risk of tip breakage. After the size of the tip end was reduced below 100 μm, a 600-grid

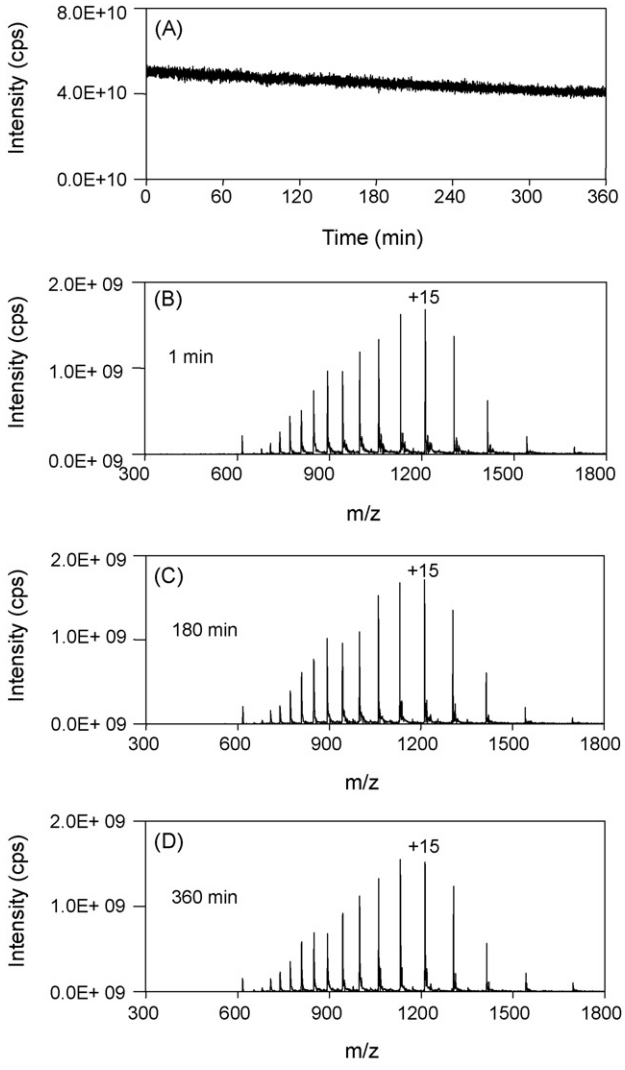

Fig. 5. Recording of TIC vs. time for 10 μM myoglobin in a period of 360 min (A), and mass spectra with 1-min sums recorded at 1 min (B), 180 min (C) and 360 min (D). Conditions: sample solution, 10 μM myoglobin in 50% methanol containing 1% acetic acid; infusion flow rate, 200 nL/min; ESI voltage, 2.5 kV.

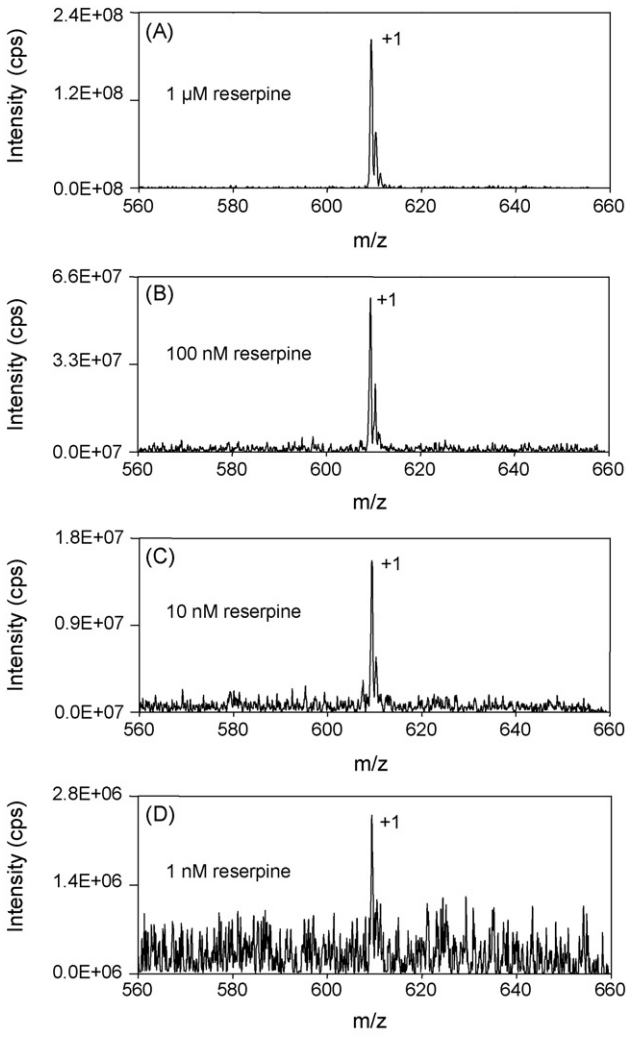

Fig. 6. Mass spectra of 1000 nM (A), 100 nM (B), 10 nM (C) and 1 nM (D) reserpine solutions in 50% methanol containing 1% acetic acid. Infusion flow rate, 200 nL/min; ESI voltage, 2.4 kV.

sandpaper instead of the 300-grid one was used to grind the tip, in order to minimize the impact of the grinding on the tip end and protect the tip end from breakage. In addition to the protecting effect, the use of high grid sandpapers also reduced the removal rate of the grinding, which allowed various tip structures, such as puncher-shaped and fork-shaped tips, to be easily fabricated. After the fabrication for the main structure of the tip was completed, a 2000-grid sandpaper was used mainly to polish the tip outer surface.

With the fabrication approach described above, the phenomenon of the tip end breakage rarely happened in the fabrication process for more than 20 chips. In this work, the fabrication of the tip was carried out manually with an average fabrication time of 30 min for each tip. The fabrication speed and yield might be further increased using automatic polishing machine.

The previous studies on electrospray indicated a definite correlation between the tip structure and the stability of electrospray [40]. We examined the spray performance of the on-chip emitters and the home-made pulled capillary emitter with similar tip end size at the flow rate of 50 nL/min. For the on-chip emitter with a puncher-shaped tip end (Fig. 4A1) and the capillary emitter, stable spray could not be achieved. The relative standard deviation (RSD) of the total ion current (TIC) was 23.8% (Fig. 4A3) for the puncher-shaped tip and 96.8% (Fig. 4C) for the capillary tip. This could be attributed to the relatively large sizes of Taylor cones at the tip ends of the two emitters (Fig. 4A2). Based on the tip with a puncher-shaped tip end, we further ground the both sidewalls of the tip end to produce a sharp tip end with a fork-shaped configuration (see Fig. 4B1). At the tip end, the right and left walls of the microchannel were removed, leaving an upper and lower glass tip extending beyond the channel orifice with an end size of *ca.* 15 μm × 50 μm. The size of Taylor cone at this tip was significantly decreased (Fig. 4B2) compared with those at the puncher-shaped tips. An outstanding stability of 4.4% RSD was achieved (see Fig. 4B3), which demonstrated the feasibility of this type of emitter in nanospray-MS.

3.4. Analytical performance

The longtime stability of the LMA electrode was tested in a continuous electrospray experiment for over 6 h. Fig. 5A–D shows the recordings of TIC and mass spectrums of 1-min sum of 35 scans recorded each 3 h during the experiment. The TIC signal is quite stable, and the mass spectrums of myoglobin show identical charge distributions without loss in signal-to-noise ratio during the period. Actually, the LMA electrode had been used in one-month experiments without observable deterioration in either appearance or electrospray performance. Furthermore, if necessary, the LMA electrode could be easily regenerated using heating and remolding methods.

The detection sensitivity of the present chip-ESI-MS system with the fork-shaped tip was measured with 1, 10, 100 and 1000 nM reserpine solutions. The mass spectrums are as shown in Fig. 6A–D, and each spectrum was obtained in 0.4 s without data average. The peak of single charge reserpine at 609 m/z could be clearly observed in the spectrum of 1 nM reserpine solution (Fig. 6D), which indicated that the limit of detection was lower than 1.4 amol reserpine. The high sensitivity could be partially attributed to the low background generated by the present glass emitter. In addition, considering that the LMA material is more active in chemical and electrochemical properties than those of gold or platinum, which may result in interference to MS analysis by the electrode corrosion, a comparison experiment was performed using a commercial nanospray tip and a blank solution (50% methanol, see Fig. S1 in supplementary data for detail). The results showed no significant difference in background signal between the present system and the commercial nanospray tip, which indicated that there was no

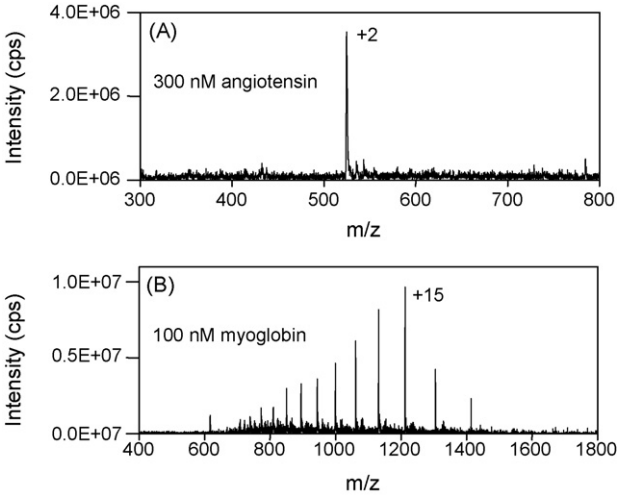

Fig. 7. Mass spectra of 300 nM human angiotensin II (A) and 100 nM myoglobin (B). Infusion flow rate, 200 nL/min; ESI voltage, 2.5 kV.

detectable contamination originated from either the glass substrate or the LMA electrode.

The feasibility of the present chip-ESI-MS system in the analysis of peptides and proteins was also demonstrated in the determination of 300 nM human angiotensin II and 100 nM horse myoglobin (Fig. 7A–B). The mass spectrum of angiotensin II shows a signal-to-noise ratio of *ca.* 25 in the 2+ charge state (Fig. 7A). The multiply charged molecular ions of myoglobin ranged from 13+ to 28+, while the signal-to-noise ratio of the 15+ peak was 50, as shown in Fig. 7B.

4. Conclusions

The monolithic emitter presented here for the combination of ESI-MS with glass chip has several advantages including: (1) The fabrication process for the emitter is simple, rapid and low cost without the need of complicated and expensive instruments, and could be easily performed in routine laboratories; (2) The emitter proved to be durable and stable in the MS analysis, which is expected to be useful in long-term monitoring, such as organic synthesis and biological reactions; (3) The use of glass to produce chip-based emitters is in favor of minimizing the MS detection background [30], and thus increasing the detection sensitivity. This implies that the application of the present chip-MS system may be extended to the identification of low-abundance species, such as the analytes in proteomics and metabolomics. Additionally, the present emitter also has the potential to be used as an interface between MS and other analysis systems on microchip, such as capillary electrophoresis, liquid chromatography and high-throughput droplet analysis.

The present fabrication technique for the LMA electrode provided a simple approach to produce metal electrode on microchip with direct electrode–solution contact without the need of complicated fabrication processes or chemical treatments on the channel surface. It could be applied not only in chip-ESI-MS, but also in microchips with other electric components, such as electrochemical sensors, dielectric manipulation of cells or droplets, and electrolysis pump. Although glass chips were used in the present system to demonstrate the feasibility of the LMA electrode, the present fabrication technique could be readily applied in microchips produced from other materials, such as quartz or plastic.

Compared with the commercial capillary nanospray tips, the size of tips described in this work is still relatively larger. The further decrease of the chip tip size is limited by the channel size fabricated by the wet isotropic etching technique. This problem could be solved using dry etching technique to fabricate the microchannel, which should help to reduce the tip dimension, and thereby enhance the analytical performance of the present emitter.

Acknowledgments

Financial supports from National Natural Science Foundation of China (Grants 20775071, 20825517, and 20890020) and Major State Basic Research Development Program of China (Grants 2007CB714503 and 2007CB914100) are gratefully acknowledged.

Appendix A. Supplementary data

Supplementary data associated with this article can be found, in the online version, at doi:10.1016/j.talanta.2010.01.064.

References

[1] G.M. Whitesides, Nature 442 (2006) 368–373.
[2] D. Janasek, J. Franzke, A. Manz, Nature 442 (2006) 374–380.
[3] Z.H. Liang, N. Chiem, G. Ocvirk, T. Tang, K. Fluri, D.J. Harrison, Anal. Chem. 68 (1996) 1040–1046.
[4] J.L. Fu, Q. Fang, T. Zhang, X.H. Jin, Z.L. Fang, Anal. Chem. 78 (2006) 3827–3834.
[5] A.T. Woolley, K.Q. Lao, A.N. Glazer, R.A. Mathies, Anal. Chem. 70 (1998) 684–688.
[6] S. Koster, E. Verpoorte, Lab Chip 7 (2007) 1394–1412.
[7] I.M. Lazar, J. Grym, F. Foret, Mass Spectrom. Rev. 25 (2006) 573–594.
[8] Q.F. Xue, F. Foret, Y.M. Dunayevskiy, P.M. Zavracky, N.E. McGruer, B.L. Karger, Anal. Chem. 69 (1997) 426–430.
[9] R.S. Ramsey, J.M. Ramsey, Anal. Chem. 69 (1997) 1174–1178.
[10] D. Figeys, Y.B. Ning, R. Aebersold, Anal. Chem. 69 (1997) 3153–3160.
[11] I.M. Lazar, R.S. Ramsey, S. Sundberg, J.M. Ramsey, Anal. Chem. 71 (1999) 3627–3631.
[12] B. Zhang, H. Liu, B.L. Karger, F. Foret, Anal. Chem. 71 (1999) 3258–3264.
[13] J.J. Li, P. Thibault, N.H. Bings, C.D. Skinner, C. Wang, C. Colyer, J. Harrison, Anal. Chem. 71 (1999) 3036–3045.
[14] J.J. Li, J.F. Kelly, I. Chemushevich, D.J. Harrison, P. Thibault, Anal. Chem. 72 (2000) 599–609.
[15] H.H. Liu, C. Felten, Q.F. Xue, B.L. Zhang, P. Jedrzejewski, B.L. Karger, F. Foret, Anal. Chem. 72 (2000) 3303–3310.
[16] J. Gao, J. Xu, L.E. Locascio, C.S. Lee, Anal. Chem. 73 (2001) 2648–2655.
[17] B.L. Zhang, F. Foret, B.L. Karger, Anal. Chem. 73 (2001) 2675–2681.
[18] Y.Z. Deng, J. Henion, J.J. Li, P. Thibault, C. Wang, D.J. Harrison, Anal. Chem. 73 (2001) 639–646.
[19] S. Ssenyange, J. Taylor, D.J. Harrison, M.T. McDermott, Anal. Chem. 76 (2004) 2393–2397.
[20] H.L. Wu, Y.P. Tian, B.H. Liu, H.J. Lu, X.Y. Wang, J.J. Zhai, H. Jin, P.Y. Yang, Y.M. Xu, H.H. Wang, J. Proteome. Res. 3 (2004) 1201–1209.
[21] X.D. Cao, Q. Fang, Z.L. Fang, Chem. J. Chinese U. 25 (2004) 1231–1234.
[22] C.H. Yuan, J. Shiea, Anal. Chem. 73 (2001) 1080–1083.
[23] Y.N. Yang, C. Li, J. Kameoka, K.H. Lee, H.G. Craighead, Lab Chip 5 (2005) 869–876.
[24] R.T. Kelly, K. Tang, D. Irimia, M. Toner, R.D. Smith, Anal. Chem. 80 (2008) 3824–3831.
[25] M. Svedberg, A. Pettersson, S. Nilsson, J. Bergquist, L. Nyholm, F. Nikolajeff, K. Markides, Anal. Chem. 75 (2003) 3934–3940.
[26] M. Svedberg, M. Veszelei, J. Axelsson, M. Vangbo, F. Nikolajeff, Lab Chip 4 (2004) 322–327.
[27] K. Tang, Y. Lin, D.W. Matson, T. Kim, R.D. Smith, Anal. Chem. 73 (2001) 1658–1663.
[28] M. Schilling, W. Nigge, A. Rudzinski, A. Neyer, R. Hergenroder, Lab Chip 4 (2004) 220–224.
[29] M.F. Bedair, R.D. Oleschuk, Anal. Chem. 78 (2006) 1130–1138.
[30] J.S. Kim, D.R. Knapp, J. Am. Soc. Mass. Spectrom. 12 (2001) 463–469.
[31] P. Hoffmann, U. Hausig, P. Schulze, D. Belder, Angew. Chem., Int. Ed. 46 (2007) 4913–4916.
[32] G.E. Yue, M.G. Roper, E.D. Jeffery, C.J. Easley, C. Balchunas, J.P. Landers, J.P. Ferrance, Lab Chip 5 (2005) 619–627.
[33] J.S. Mellors, V. Gorbounov, R.S. Ramsey, J.M. Ramsey, Anal. Chem. 80 (2008) 6881–6887.
[34] A.C. Siegel, S.S. Shevkoplyas, D.B. Weibel, D.A. Bruzewicz, A.W. Martinez, G.M. Whitesides, Angew. Chem., Int. Ed. 45 (2006) 6877–6882.
[35] Q. Fang, G.M. Xu, Z.L. Fang, Anal. Chem. 74 (2002) 1223–1231.
[36] Z.J. Jia, Q. Fang, Z.L. Fang, Anal. Chem. 76 (2004) 5597–5602.
[37] Q.H. He, Q. Fang, W.B. Du, Z.L. Fang, Electrophoresis 28 (2007) 2912–2919.
[38] T. Zhang, Q. Fang, W.B. Du, J.L. Fu, Anal. Chem. 81 (2009) 3693–3698.
[39] A. Hibara, S. Iwayama, S. Matsuoka, M. Ueno, Y. Kikutani, M. Tokeshi, T. Kitamori, Anal. Chem. 77 (2005) 943–947.
[40] Y.Z. Chang, Y.R. Chen, G.R. Her, Anal. Chem. 73 (2001) 5083–5087.